Neurotoxicity Research (2019) 35:475–483
https://doi.org/10.1007/s12640-018-9976-1

ORIGINAL ARTICLE

Guanosine Protects Striatal Slices Against 6-OHDA-Induced Oxidative Damage, Mitochondrial Dysfunction, and ATP Depletion

Naiani Ferreira Marques[1] · Caio Marcos Massari[1] · Carla Inês Tasca[1,2]

Received: 3 July 2018 / Revised: 26 October 2018 / Accepted: 30 October 2018 / Published online: 12 November 2018

Abstract

Parkinson's disease (PD) is a progressive neurodegenerative disorder characterized by loss of dopaminergic neurons in *substantia nigra pars compacta* which induces severe motor symptoms. 6-OHDA is a neurotoxin widely used in PD animal models due to its high affinity by dopamine transporter, its rapid non-enzymatic auto-oxidation which generates reactive oxygen species (ROS), oxidative stress, and for induced mitochondrial dysfunction. We previously reported an in vitro protocol of 6-OHDA-induced toxicity in brain regions slices, as a simple and sensitive assay to screen for protective compounds related to PD. Guanosine (GUO), a guanine-based purine nucleoside, is a neuroprotective molecule that is showing promising effects as an antiparkinsonian agent. To investigate the mechanisms involved on GUO-induced neuroprotection, slices of cortex, striatum, and hippocampus were incubated with GUO in the presence of 6-OHDA (100 μM). 6-OHDA promoted a decrease in cellular viability and increased ROS generation in all brain regions. Disruption of mitochondrial potential, depletion in intracellular ATP levels, and increase in cell membrane permeabilization were evidenced in striatal slices. GUO prevented the increase in ROS generation, disruption in mitochondrial potential, and depletion of intracellular ATP induced by 6-OHDA in striatal slices. In conclusion, GUO was effective to prevent oxidative events before cell damage, such as mitochondrial disruption, intracellular ATP levels depletion, and ROS generation in striatal slices subjected to in vitro 6-OHDA-induced toxicity.

Keywords Parkinson's disease · 6-OHDA · Guanosine · In vitro

Abbreviations

6-OHDA	6-Hydroxydopamine
GUO	Guanosine
KRB	Krebs–Ringer buffer
MTT	3-(4,5-dimethylthiazol-2-yl)-2,5-diphenyltetrazolium bromide
DMSO	Dimethyl sulfoxide
DCFH-DA	Dichlorodihydrofluorescein diacetate
DCFH	Dichlorodihydrofluorescein
DCF	Dichlorofluorescein
FCCP	Carbonyl cyanide 4-(trifluoromethoxy)-phenylhydrazone
PD	Parkinson's disease
ROS	Reactive oxygen species
TMRE	Tetramethylrhodamine ethyl ester
PI	Propidium iodide

✉ Carla Inês Tasca
carla.tasca@ufsc.br

[1] Programa de Pós-Graduação em Bioquímica, Centro de Ciências Biológicas, Universidade Federal de Santa Catarina, Florianópolis, Santa Catarina, Brazil

[2] Departamento de Bioquímica, CCB, UFSC, Trindade, Florianópolis, Santa Catarina 88040-900, Brazil

Introduction

Parkinson's disease (PD) is an age-associated neurodegenerative disorder affecting 1–2% of people aged over 65 years and 4% of people aged over 85, characterized by a loss of dopaminergic neurons in the *substantia nigra pars compacta* (SNpc) leading to a subsequent depletion of dopamine in the striatum (de Lau and Breteler 2006). Also, other neurotransmitters and other brain areas are involved in the pathophysiology of this disease, including the hippocampus and cerebral cortex (Braak et al. 2004). Even though the neuropathological hallmarks of PD are well described, the specific biochemical mechanism responsible for the degeneration and disease progression remains unclear. Notably, studies suggest that

mitochondrial dysfunction is a relevant target in PD pathogenesis (Bose and Beal 2016).

Mitochondria is the main source of ATP production, essential for the survival and maintenance of neurons, and protein phosphorylation reactions that mediate synaptic signaling in neuronal function (Parker et al. 1989). Alterations in mitochondrial complexes of the respiratory chain have a direct impact on the overall energy state of the cell. A deficiency in complex I activity (about 35% of activity reduction) was described in *post-mortem* studies in the *substantia nigra* and cortex of PD patients (Mizuno et al. 1989; Navarro et al. 2009).

PD studies are mainly reported using toxins designed to mimic the neurodegeneration in the nigrostriatal pathway. 6-hydroxydopamine (6-OHDA) induces dopaminergic degeneration due to a high affinity for the dopaminergic transporter (Garver et al. 1975). Once inside the neuron, 6-OHDA crosses mitochondrial membranes and inhibit the complex I activity in the electron transport chain (Perier and Vila 2012). Also, 6-OHDA can accumulate in the cytosol, where it undergoes a non-enzymatic auto-oxidation, promoting reactive oxygen species (ROS) formation (Blandini et al. 2008). In vitro evaluation of 6-OHDA toxicity showed it directly inhibits mitochondrial complex I and IV, without involving a free-radical mechanism (Glinka and Youdim 1995). This effect might be an earlier toxic event followed by free radicals toxicity in the cytosol, which occurs lately and probably is responsible for lipid peroxidation in vitro. Therefore, 6-OHDA causes respiratory inhibition and oxidative stress, and both toxic mechanisms are not necessarily linked, but appear to act synergistically during neuron degeneration (Schober 2004). Due to these effects, 6-OHDA is one of the most used toxins for PD models and is a great tool for screening possible neuroprotective agents (Kostrzewa and Jacobowitz 1974; Segura-Aguilar and Kostrzewa 2015).

Several studies have shown that guanosine (GUO) protects against toxic events in the central nervous system (CNS), manly attenuating excitotoxicity and mitochondrial damage (Thomaz et al. 2016; Dal-Cim et al. 2012; Dobrachinski et al. 2017). In a parkinsonism rodent model induced by a proteasome inhibitor, GUO showed protective effects against neuronal apoptotic cell death, increased tyrosine hydroxylase-positive cells in the SNpc with consequent improvement in motor function (Su et al. 2009). In this model, it was also demonstrated that GUO induced cellular proliferation in the SNpc and subventricular zone and increased expression of fibroblast growth factor. These results point to GUO as a promising therapeutic strategy in neurodegenerative disease, and specifically in PD.

Our group established a 6-OHDA-induced toxicity protocol in brain slices as an in vitro model, to evaluate neuroprotective agents related to PD. We showed that in vitro incubation with 6-OHDA induced increase in ROS generation, decrease in cellular viability in the cortical, striatal, and hippocampal slices, and disruption in mitochondrial membrane potential in the cortex and striatum (Massari et al. 2016). Oxidative stress is reported as an important factor in early biochemical events in the pathogenesis of PD, before cell death and neurodegeneration process advance (Dias et al. 2013; Poewe et al. 2017). In the present study, we improved information on this new in vitro protocol of evaluating 6-OHDA-induced toxicity, by showing there is a selective loss of mitochondrial membrane potential and depletion of ATP levels in the striatal slices, followed by an increased cellular membrane permeabilization. Additionally, GUO prevented 6-OHDA-induced mitochondrial stress and ATP depletion in the striatal slices, displaying its protective effect against a PD-related toxin.

Materials and Methods

Animals

Male *Wistar* rats (3 months old, 350–400 g) were obtained for local colony, maintained in a 12-h dark/light cycle, at constant room temperature at 23 ± 1 °C and with food and water *ad libitum*. Experiments followed the "The ARRIVE Guidelines" published in 2010 and were approved by the local Ethical Committee for Animal Research (CEUA/UFSC PP00955).

Preparation of Brain Slices

Animals were euthanized and the whole brain was quickly removed and placed on ice. The cortex, striatum, and hippocampus were rapidly dissected in ice-cold Krebs–Ringer buffer (KRB) (122 mM NaCl, 3 mM KCl, 1.2 mM $MgSO_4$, 1.3 mM $CaCl_2$, 0.4 mM KH_2PO_4, 25 mM $NaHCO_3$, and 10 mM D-glucose, bubbled with 95% CO_2/ 5% O_2 up to pH 7.4). Slices (0.4 mm) were prepared using a McIlwain Tissue Chopper (The Mickle Laboratory Engineering Co. ltd., England) and separated in KRB at 4 °C. After sectioning, slices were incubated in 500 μL of KRB for each slice for 30 min, at 37 °C, for recovery from trauma slicing before starting the experiment.

Slices Treatment

6-OHDA (Sigma, St. Louis, MO, USA) was diluted in water at 0.1% sodium metabisulfite for avoiding oxidation and stored at – 20 °C. For the experiment, 6-OHDA was diluted at 100 μM in KRB. To investigate 6-OHDA-induced damage, one slice from each brain region was selected and exposed to 6-OHDA (100 μM) during 1 h (Massari et al. 2016). GUO (Sigma, St. Louis, MO, USA) was diluted in KRB (at 30, 100, or 300 μM) and co-incubated with 6-OHDA for 1 h to determine its potential neuroprotective effect. Slices of control

group were incubated in a physiological KRB at 500 μL for each slice. All experiments were performed in triplicates. After the 1 h of co-incubation with 6-OHDA and GUO, ROS production, mitochondrial membrane potential, intracellular ATP levels, and membrane permeability were evaluated. In another set of experiments, following 6-OHDA + GUO co-incubation, slices were maintained for additional 3 h in a nutritive culture medium (DMEM/F12) composed of 50% KRB, 50% DMEM, and 20 mM HEPES, at 37 °C in a CO_2 atmosphere (Molz et al. 2008). After 3 h, cellular viability and membrane permeability parameters were assessed.

Cellular Viability and Membrane Integrity Evaluation

Cellular viability in the cortical, striatal, and hippocampal slices was quantified by measuring the reduction of 3-(4,5-dimethylthiazol-2-yl)-2,5-diphenyltetrazolium bromide (MTT) to a dark violet formazan product by mitochondrial dehydrogenases (Mosmann 1983; Liu et al. 1997). After 1 h of co-incubation with 6-OHDA and GUO and additional 3 h in culture medium, cellular viability was assessed. Slices were incubated with 500 μL of MTT (0.5 mg/mL) in KRB buffer for 20 min at 37 °C, and the formazan produced was solubilized by replacing the medium with 0.2 mL of dimethylsulfoxide (DMSO), resulting in a colored compound which was quantified spectrophotometrically at a wavelength of 550 nm.

Membrane integrity was assessed by evaluating uptake of the fluorescent exclusion dye propidium iodide (PI, Sigma-Aldrich, St Louis, MO, USA). PI is a polar compound that enters only in cells with damaged membranes. Once inside the cells, PI complexes with DNA and emits an intense red fluorescence (630 nm) when excited by green light (495 nm). Following GUO and 6-OHDA co-incubation (1 h) or GUO and 6-OHDA co-incubation plus 3 additional hours in the nutritive culture medium, slices were incubated with 500 μL of PI (7 μg/ml) and maintained for 30 min at 37 °C, and then washed with KRB for analysis on a fluorescence microplate reader TECAN (Tecan Group Ltd., Mannedorf, Switzerland) (Piermartiri et al. 2009).

ROS Generation and Mitochondrial Membrane Potential

ROS generation was measured by using the molecular probe 2,7-dichlorodihydrofluorescein diacetate (DCFH-DA, Sigma-Aldrich, St Louis, MO, USA), which diffuses through the cell membrane and is hydrolyzed by intracellular esterases to the non-fluorescent form dichlorodihydrofluorescein (DCFH). DCFH reacts with intracellular ROS to form dichlorofluorescein (DCF), a green fluorescent dye. DCF fluorescence intensity is proportional to the amount of ROS. Brain slices were incubated with 500 μL of DCFH-DA (80 μM) for 30 min at 37 °C and then washed and kept in KRB. Fluorescence was measured in one slice from brain regions, assayed in triplicates, using excitation and emission wavelengths of 480 and 525 nm, respectively.

Mitochondrial membrane potential was measured using the molecular probe tetramethylrhodamine ethyl ester (TMRE, Sigma-Aldrich, St Louis, MO, USA) (100 nM) for 30 min at 37 °C (Egea et al. 2007). Fluorescence was measured using wavelengths of excitation and emission of 550 and 590 nm, respectively. Results were obtained as relative fluorescence units (RFU) from individual experiments. RFU variation among the experiments was normalized by expressing data as means and SEM of percentage relative to controls. Both ROS generation and mitochondrial membrane potential measurements were carried out after 1 h of GUO + 6-OHDA co-incubation.

Intracellular ATP Levels

After GUO and 6-OHDA co-treatment, the brain cortical, striatal, and hippocampal slices were homogenized in 320 μL of trichloroacetic acid (TCA) 2% aqueous solution. The homogenates were centrifuged at 14,000 rpm at 4 °C for 3 min. The supernatants were used for determination of ATP levels using a bioluminescent assay kit (catalog code FLAA) according to the manufacturer's recommendations (Sigma-Aldrich, St Louis, MO, USA). Triplicates of 100 μL from the supernatant were incubated with the mix assay and ATP levels measured after 3 min of incubation at room temperature. The amount of protein in each sample was quantified using the method of (Lowry et al. 1951) and the results are expressed in μM ATP/μg of protein in each sample (a pool of 3 slices per region). Bovine serum albumin (Sigma) was used as standard.

Statistical Analysis

Data are normalized among the experiments and represented as means and SEM of percentage of controls. Comparisons among experimental and control groups were performed by one- or two-way ANOVA followed by the Newman-Keuls post hoc test when appropriate. Statistical difference was accepted when $p < 0.05$.

Results

Cellular Viability

Previous results from our group showed that 6-OHDA (100 μM) causes an effective toxicity in brain slices (Massari et al. 2016). Now, to determine an effective GUO concentration that protects the brain slices from 6-OHDA toxicity, the cortical, striatal, and hippocampal slices were co-incubated with increasing GUO concentrations of 30, 100,

or 300 μM (Fig. 1a). As expected, we observed a decrease in cell viability in slices from the cortex, striatum, and hippocampus when incubated with 6-OHDA (Fig. 1 b, c, d). The co-incubation with GUO did not protect the cortical slices, at any concentration tested (Fig. 1b). However, in the striatal slices, we observed GUO attenuated 6-OHDA-induced reduction of cellular viability, in all GUO concentrations tested, although no statistical difference was observed among 6-OHDA and 6-OHDA + GUO groups (Fig. 1c). In the hippocampal slices, only 100 μM GUO attenuated the decreased cell viability induced by 6-OHDA, although it also did not reach statistical significance when compared to 6-OHDA group (Fig. 1d). Despite GUO effect did not reach statistical significance, attenuation (about 20%) of 6-OHDA-induced toxicity is observed. Thus, considering previous studies from our group showing a protective effect of GUO in in vitro neurotoxicity protocols (Dal-Cim et al. 2013a; Thomaz et al. 2016; Dal-Cim et al. 2011; Molz et al. 2011), next evaluations were conducted with 100 μM GUO.

ROS Generation

6-OHDA-induced toxicity is mainly attributed to a production of reactive species, mostly hydrogen peroxide (Schober 2004). Therefore, we evaluated early toxic effects of 6-OHDA as induction of ROS production (Fig. 2a). Slices incubated with 6-OHDA showed a significant increase in ROS generation in the striatum and hippocampus (Fig. 2c, d). In the cortical slices, 6-OHDA induced a slight increase in ROS generation that did not reach statistical significance (Fig. 2b). Co-incubation with GUO displayed a total reduction of ROS generation in the striatal slices (Fig. 2c). In the hippocampus, reduction of ROS generation was also observed, although a significance of $p = 0.07$ was achieved (Fig. 2c).

Mitochondrial Membrane Potential and Intracellular ATP Levels

To evaluate the mitochondrial membrane potential in slices, we used the lipophilic and slightly cationic fluorescent dye TMRE (Fig. 3a). The cortical and hippocampal slices incubated with 100 μM 6-OHDA showed no significant alterations in TMRE fluorescence when compared with control group (Fig. 3b, d). However, in the striatal slices, we observed a significant decreased of TMRE fluorescence (Fig. 3c). Decrease in fluorescence can be related to a mitochondrial membrane depolarization, as the same effect was observed when slices were incubated with carbonyl cyanide 4-(trifluoromethoxy) phenylhydrazone (FCCP, 10 μM), a mitochondrial oxidative phosphorylation uncoupler, as we previously showed (Massari et al. 2016). In the striatal slices, GUO treatment prevents the mitochondrial membrane depolarization (Fig. 3c), showing a protective effect in the mitochondrial disruption induced by 6-OHDA. Thus, in order to evaluate the effects of 6-OHDA in cellular energetic balance, we performed the measurement of intracellular levels of ATP in brain slices.

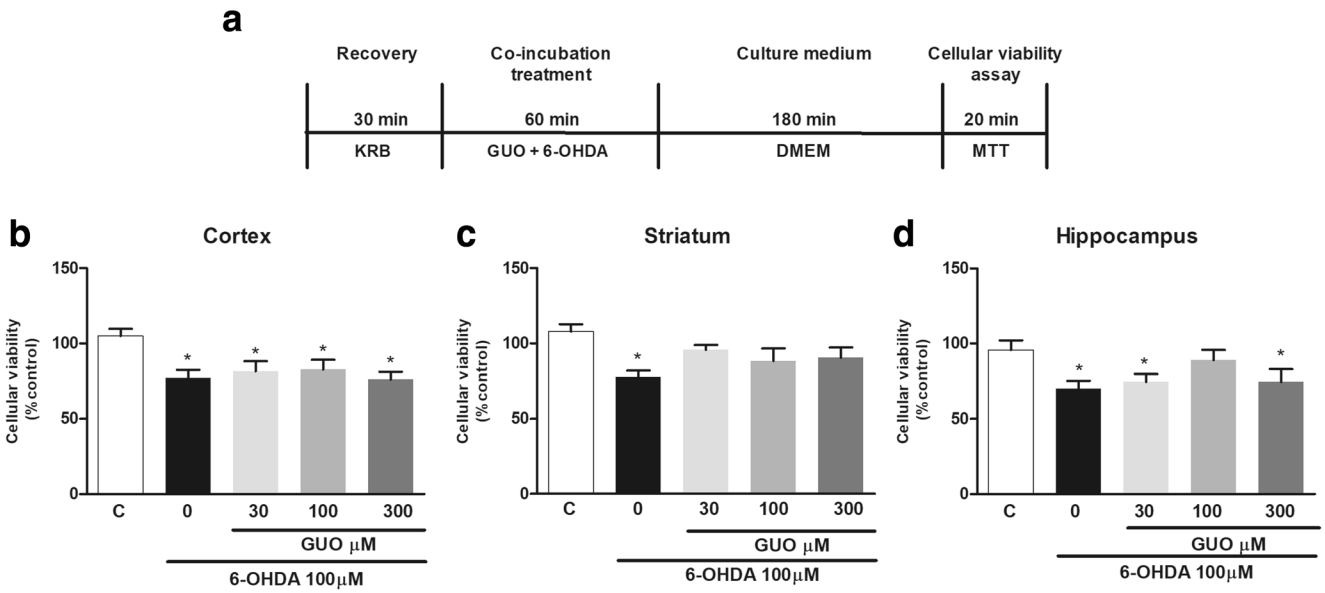

Fig. 1 Cellular viability measured in slices subjected to 6-OHDA-induced toxicity and GUO treatment in vitro. Timeline of experimental protocol in vitro (**a**) in cortical (**b**), striatal (**c**), and hippocampal (**d**) slices. Slices were co-incubated for 1 h with 100 μM 6-OHDA and GUO (30–300 μM) at 37 °C and then, the medium was changed to a fresh culture medium for 3 h. Cellular viability was measured by MTT reduction assay as described in material and methods. Data are expressed as percentage of controls normalized among individual experiments and represent means with SEM ($n = 5$). Absolute values of optical density of control groups were 2038 ± 0.15 in cortical, 1725 ± 0.34 in striatal, and 1256 ± 0.15 in hippocampal slices. $p < 0.05$ compared with control (*) or 6-OHDA (#) groups (one-way ANOVA followed by Newman-Keuls' test)

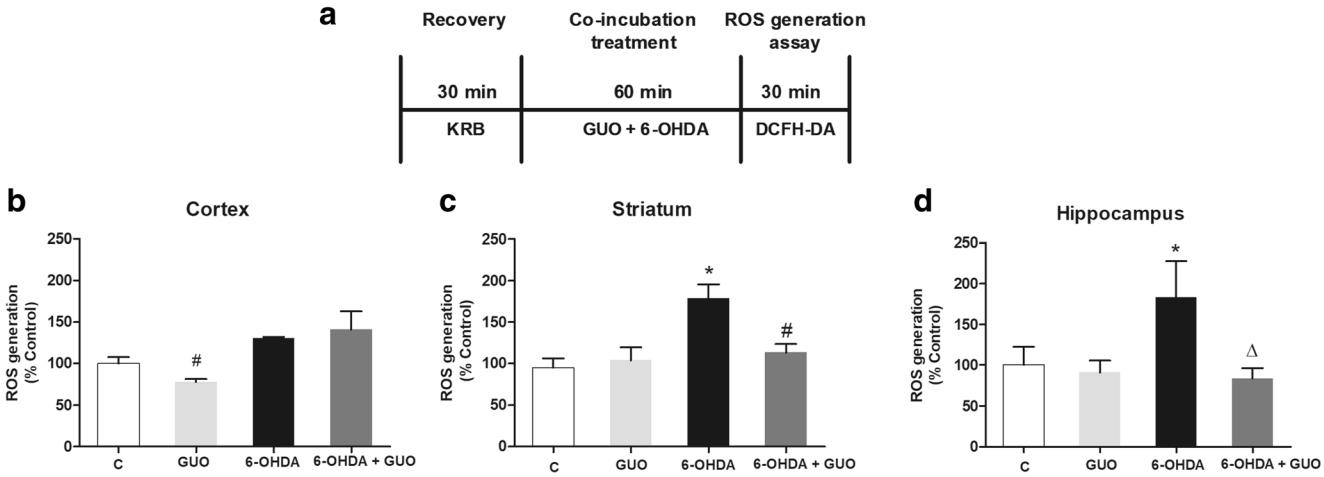

Fig. 2 ROS generation in slices subjected to 6-OHDA-induced toxicity and GUO treatment in vitro. ROS generation was measured by relative fluorescence units (RFU) of DCF probe emission. Timeline of experimental protocol in vitro (**a**) in cortical (**b**), striatal (**c**), and hippocampal (**d**) slices. Slices were co-incubated for 1 h with 100 μM 6-OHDA and 100 μM GUO at 37 °C. Data are expressed as percentage of controls normalized among individual experiments and represent means with SEM ($n = 5$). RFU for control groups were 11,247 ± 1169 in cortical, 13,953 ± 1711 in striatal, and 10,138 ± 2250 in hippocampal slices. $p = 0.07$ when compared with 6-OHDA group (Δ), and $p < 0.05$ compared with control (*) or 6-OHDA (#) groups (two-way ANOVA followed by Newman-Keuls' test)

6-OHDA induced a reduction in the intracellular ATP levels in the striatum slices, but not in the cortical and hippocampal slices (Fig. 4b, c, d). This selectivity to this damaged area is in accordance which was observed in the mitochondrial membrane potential evaluation, as mitochondrial depolarization might cause ATP depletion. Therefore, we observe mitochondrial membrane disruption and ATP depletion in the striatal slices (Fig 3 c and Fig. 4c). Importantly, GUO treatment prevented both effects in the striatum, which indicates that GUO protects brain slices against energetic unbalance induced by 6-OHDA toxicity in the mitochondrial function.

Membrane Integrity Evaluation

Following ROS generation, loss of mitochondrial potential and reduction of bioenergetics, increased cell damage might occur. Then we evaluated the membrane integrity of cells from brain slices due to the uptake of the fluorescent exclusion dye PI after 1 h of 6-OHDA and GUO co-incubation and after 1 h of co-incubation plus 3 h of maintenance in culture medium. After 1 h of incubation with 6-OHDA, we did not observe any alteration in PI incorporation in all structures (Fig. 5c, d, e). However, when evaluated 3 h after 6-OHDA

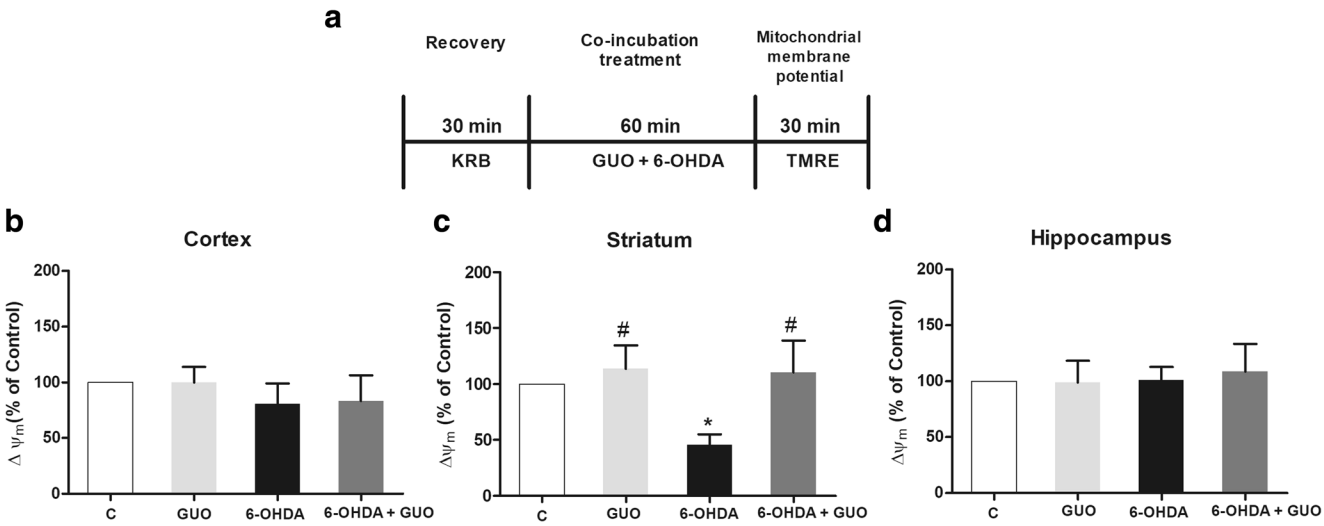

Fig. 3 Evaluation of mitochondrial membrane potential (ΔΨm) in slices subjected to 6-OHDA-induced toxicity and GUO treatment in vitro. Mitochondrial membrane potential was measured by relative fluorescence units (RFU) of TMRE probe (100 nM). Timeline of experimental protocol in vitro (**a**) in cortical (**b**), striatal (**c**) and hippocampal (**d**) slices. Slices were co-incubated for 1 h with 100 μM 6-OHDA and 100 μM GUO at 37 °C. Data are expressed as percentage of controls and represent means with SEM ($n = 5$). RFU for control groups were 303,856 ± 107,370 in cortical, 295,068 ± 130,535 in striatal, and 176,654 ± 79,006 in hippocampal slices. $p < 0.05$ compared with control (*) or 6-OHDA (#) groups (two-way ANOVA followed by Newman-Keuls' test)

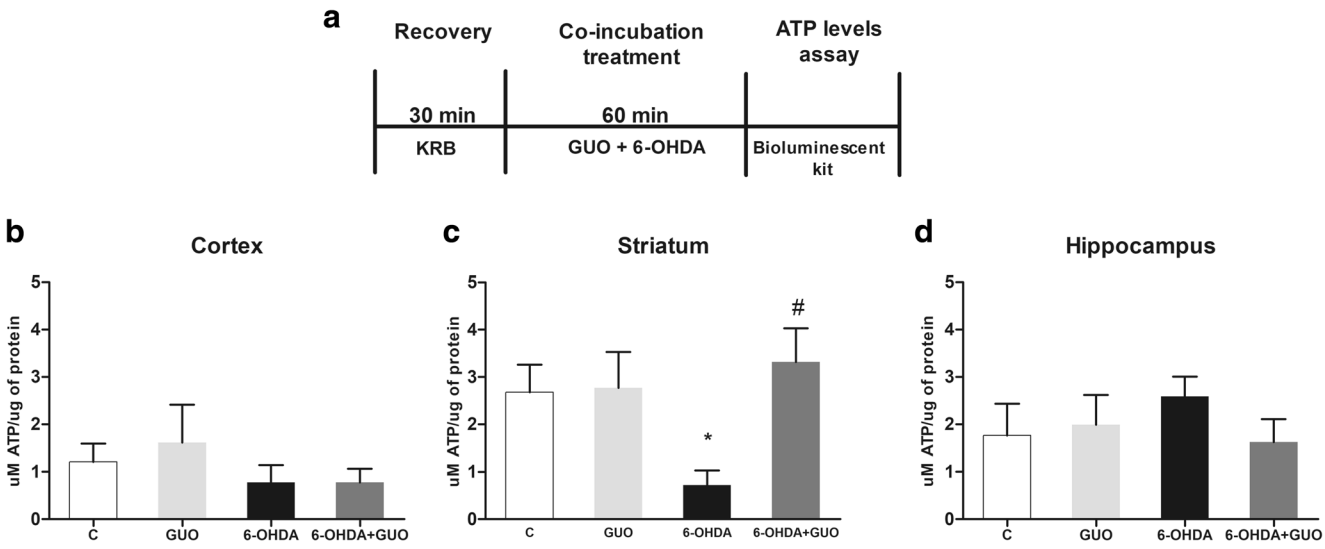

Fig. 4 Intracellular ATP levels in slices subjected to 6-OHDA-induced toxicity and GUO treatment in vitro. Timeline of experimental protocol in vitro (**a**) in cortical (**b**), striatal (**c**) and hippocampal (**d**) slices. Slices were co-incubated with 100 μM 6-OHDA and 100 μM GUO at 37 °C for 1 h. Intracellular ATP levels were measured by a bioluminescent assay kit as described in methods. Data represent means with SEM of five experiments ($n = 5$). $p < 0.05$ compared with control (*) or 6-OHDA (#) groups (two-way ANOVA followed by Newman-Keuls' test)

incubation, we observed significant increased PI incorporation in the striatum (Fig. 5d), showing that cellular membrane permeabilization needs more time to develop and be detected. GUO co-incubation with 6-OHDA promoted an attenuation of PI incorporation (about 30%) in the striatum slices, although it did not reach statistical significance ($p = 0.2096$) (Fig. 5d).

Discussion

In vitro studies have been extensively used to understand the molecular events related to neurological diseases. PD is mainly considered a motor disease due to the degeneration in dopaminergic neurons that project to the striatum and are responsible for motor function modulation. However, it is known

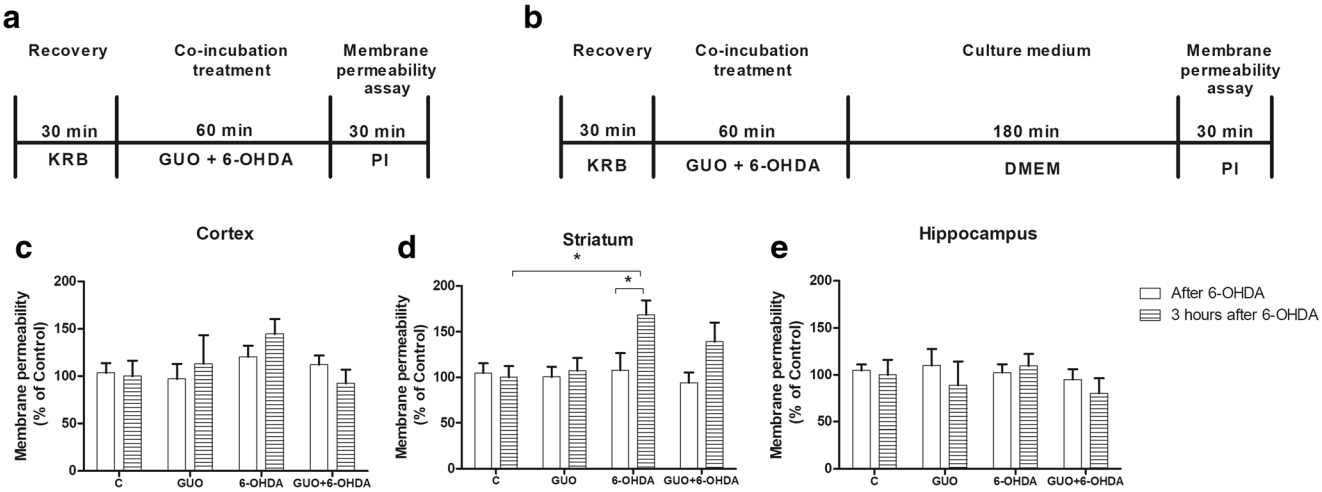

Fig. 5 Evaluation of cell membrane permeabilization by propidium iodide (PI) incorporation in slices after 1 h (**a**) or after 3 h (**b**) of co-incubation in vitro. Timeline of experimental protocol in vitro (**a** and **b**), in cortical (**c**), striatal (**d**), and hippocampal (**e**) slices. Slices were co-incubated with 100 μM 6-OHDA and 100 μM GUO at 37 °C for 1 h. In the first protocol (**a**), slices were incubated with PI (7 μg/mL) after the co-incubation, while in the second protocol (**b**), after the co-incubation, the medium was changed to a fresh culture medium (DMEM) and slices maintained for 3 h and then incubated with PI. Data expressed as percentage of controls normalized among individual experiments and represent means with SEM ($n = 5$). Relative fluorescence units (RFU) for control groups after 1 h were 25,361 ± 2744 in cortical, 29,005 ± 3222 in striatal, and 17,138 ± 1220 in hippocampal slices; and after 3 h were 15,424 ± 8369, 17,261 ± 2105, and 13,793 ± 2186 in cortical, striatal, and hippocampal slices, respectively. $p < 0.05$ compared with control group (*) (two-way ANOVA followed by Newman-Keuls' test)

that other brain areas are also involved in this disease, being affected by accumulation of α-synuclein, Lewy bodies, and other PD pathophysiology characteristics (Goedert et al. 2013; Przedborski 2017). Thus, we performed an in vitro study to evaluate 6-OHDA-induced toxicity in brain slices from regions related with molecular events during PD progression. Here, we demonstrated GUO exerts a neuroprotective effect in the striatal slices against 6-OHDA-induced biochemical changes which leads to the cell damage. 6-OHDA decreased the cellular viability in the cortical, striatal, and hippocampal slices, according to previous study from our group (Massari et al. 2016). Also, GUO (100 μM) attenuated 6-OHDA-induced damage in the hippocampal and striatal slices.

Additionally, we analyzed the PI incorporation 1 h after incubation with 6-OHDA and we did not observe any alterations in brain regions. Thus, we speculate that initial alterations in ROS generation and mitochondrial membrane potential induced by 6-OHDA incubation could lead a lipid membrane damage, which we observed in PI incorporation assay 3 h after 6-OHDA incubation in the striatum slices. Previous studies demonstrated 6-OHDA-induced lipid peroxidation in rat striatal slices at 300 μM (Cunha et al. 2014) and in PC12 cells at 100 μM (Magalingam et al. 2014). As expected, 6-OHDA increases ROS generation in brain slices from the striatum and hippocampus, we observed an increase of 30% in ROS generation in the cortex; however, this result did not show statistic difference as previously demonstrated (Massari et al. 2016). GUO 100 uM protects brain slices against ROS generation induced by 6-OHDA in the striatum and hippocampus, also protects the hippocampal slices against oxygen and glucose deprivation (Thomaz et al. 2016). This increase in ROS generation can be due the auto-oxidation of 6-OHDA in cellular cytosol, as well as the disruption of the energetic metabolism by the inhibition of complex I in the mitochondria (Blandini et al. 2008), both related with aging and neurodegenerative disease. It was also showed that 6-OHDA can generate hydroxyl radicals (OH) which can react with deoxyguanosine (Herraiz and Galisteo 2015). Then, one might speculate that the mechanism of GUO protection against 6-OHDA could be due to interaction with free radicals generated by 6-OHDA. However, we recently demonstrated that GUO did not present scavenger activity against the 2,2-diphenyl-1-picrylhydrazyl (DPPH) radical at different concentrations (Thomaz et al. 2016).

Regarding the effects of 6-OHDA in the mitochondrial membrane potential, we observed a restrict disruption in the striatum. Previous studies have shown differences in toxic effects between brain regions due to the difference of dopamine transporter (DAT) expression (Block et al. 2015; Hong et al. 2015). Whereas the striatum presented a major expression of DAT when compared with the hippocampus and cortex (Block et al. 2015), which would cause a lower accumulation of the toxin in the intracellular space in these regions compared with the striatum. Decreased TMRE fluorescence observed can be interpreted as a mitochondrial membrane depolarization, since FCCP (a mitochondrial oxidative phosphorylation uncoupler) produces similar results (Massari et al.

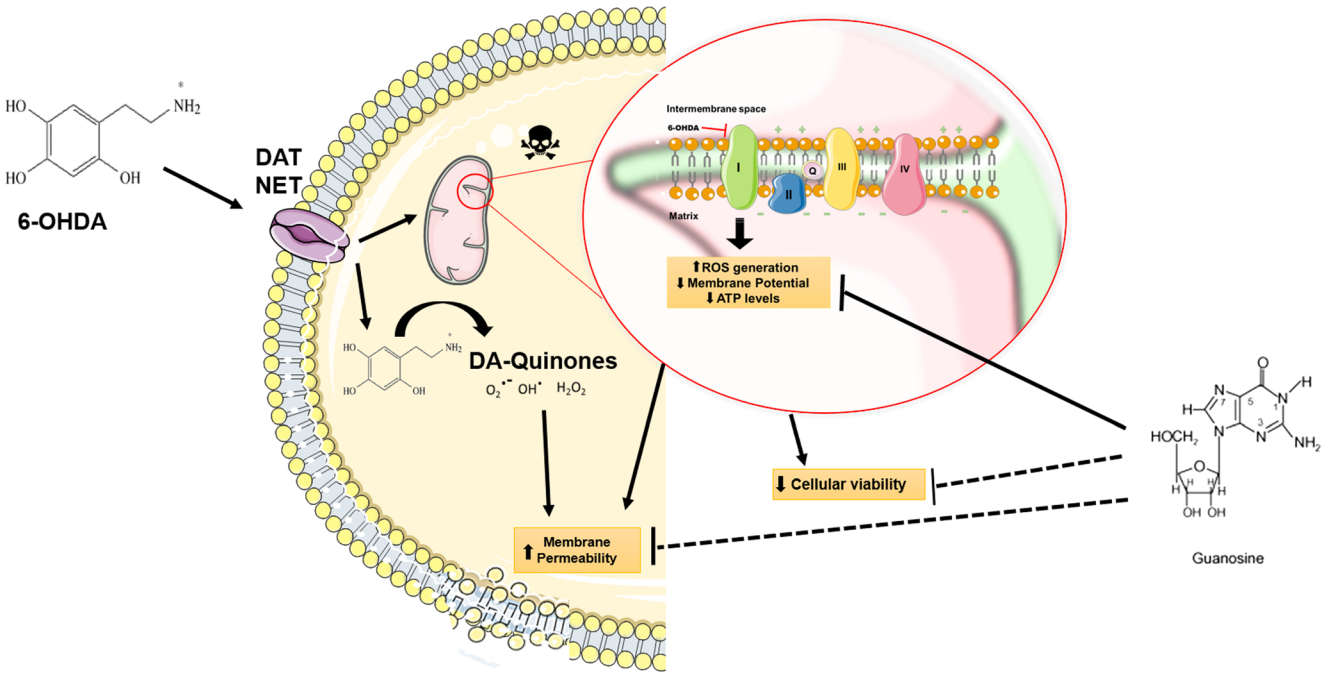

Fig. 6 Proposed mechanism of neuroprotection afforded by GUO against 6-OHDA toxicity in vitro in striatal slices. 6-OHDA increases ROS generation and membrane permeability, besides causing a decrease in ATP levels and loss of mitochondrial membrane potential. Guanosine protects striatal slices against oxidative damage, mitochondrial dysfunction, and ATP depletion evoked by in vitro 6-OHDA-induced toxicity. Guanosine also attenuates membrane permeability and cellular viability alterations induced by 6-OHDA (dashed arrow)

2016). Once again, GUO protects the striatum slices, maintaining the normal mitochondrial membrane potential.

Guanosine in vitro exerts neuroprotective effect by regulating mitochondrial function and nitroxidative stress in an ischemic-like in vitro protocol (Thomaz et al. 2016; Dal-Cim et al. 2012; Dal-Cim et al. 2013b). These effects of guanosine were accompanied by prevention of damaging modulators that are active during an oxidative situation, such as reduction of the transcription factor NFκ-B and inducible nitric oxide synthase expressions (Dal-Cim et al. 2013a). Dysfunction in the mitochondrial respiratory chain and oxidative stress can also lead to reduction in ATP production. Therefore, we evaluated the intracellular ATP in brain regions and observed that GUO protects the striatal slices from 6-OHDA-induced ATP depletion. Then, GUO protects mitochondrial membrane potential and functionality by the capability of maintenance of intracellular ATP levels in the striatal slices.

Although the exact mechanisms of action of GUO are still not completely elucidated, this purine has clearly been shown to exert therapeutic potential, acting as a neuromodulator in experimental models of several brain disorders. The neuroprotective effect seems to be mainly due to capacity of modulating and protecting against cellular toxic mechanisms such as glutamatergic excitotoxicity, oxidative, nitroxidative stress, and mitochondrial disruption (Lanznaster et al. 2016). Some of these protective effects are dependent of adenosine receptors modulation and MAPK/ERK signaling pathways (Dal-Cim et al. 2013b). Further experiments are necessary to understand the mechanisms of GUO in this 6-OHDA-induced toxicity in vitro. Besides these in vitro evaluations, recently, we reported GUO showed promising results in in vivo studies, being effective to reverse motor deficits in two animal models of PD. GUO orally administered to mice or rats protected against reserpine-induced catalepsy, tremulous jaw movements, and L-DOPA-induced dyskinesia (Massari et al. 2017).

In summary, we observed a selective toxicity of 6-OHDA in the striatal slices from rats as compared with the cortical and hippocampal slices in vitro. In the striatal slices, 6-OHDA induces an increase in ROS generation, a decrease of cellular viability, a disruption in mitochondrial membrane potential, a depletion of intracellular ATP levels, and an increase in cellular membrane permeability. GUO protects the striatal slices against increased ROS generation, disruption of mitochondrial membrane potential, and depletion in intracellular ATP levels (Fig. 6). Guanosine prevents some of the cellular toxic events induced by 6-OHDA, protecting against disruption of mitochondrial-related process.

Funding Information Research supported by grants from the Brazilian funding agencies, CAPES (CAPES/PAJT), CNPq (INCT-EN for Excitotoxicity and Neuroprotection) and FAPESC (NENASC/PRONEX) to C.I.T. is recipient of CNPq productivity fellowship.

Compliance with Ethical Standards

Experiments followed the "The ARRIVE Guidelines" published in 2010 and were approved by the local Ethical Committee for Animal Research (CEUA/UFSC PP00955).

References

Blandini F, Armentero MT, Martignoni E (2008) The 6-hydroxydopamine model: news from the past. Parkinsonism Relat Disord 14(Suppl 2):S124–S129. https://doi.org/10.1016/j.parkreldis.2008.04.015

Block ER, Nuttle J, Balcita-Pedicino JJ, Caltagarone J, Watkins SC, Sesack SR, Sorkin A (2015) Brain region-specific trafficking of the dopamine transporter. J Neurosci 35(37):12845–12858. https://doi.org/10.1523/JNEUROSCI.1391-15.2015

Bose A, Beal MF (2016) Mitochondrial dysfunction in Parkinson's disease. J Neurochem 139(Suppl 1):216–231. https://doi.org/10.1111/jnc.13731

Braak H, Ghebremedhin E, Rüb U, Bratzke H, Del Tredici K (2004) Stages in the development of Parkinson's disease-related pathology. Cell Tissue Res 318(1):121–134. https://doi.org/10.1007/s00441-004-0956-9

Cunha MP, Martín-de-Saavedra MD, Romero A, Egea J, Ludka FK, Tasca CI, Farina M, Rodrigues ALS, López MG (2014) Both creatine and its product phosphocreatine reduce oxidative stress and afford neuroprotection in an in vitro Parkinson's model. ASN Neuro 6(6):175909141455494. https://doi.org/10.1177/1759091414554945

Dal-Cim T, Ludka FK, Martins WC, Reginato C, Parada E, Egea J, López MG, Tasca CI (2013a) Guanosine controls inflammatory pathways to afford neuroprotection of hippocampal slices under oxygen and glucose deprivation conditions (research support, non-U.S. Gov't). J Neurochem 126(4):437–450. https://doi.org/10.1111/jnc.12324

Dal-Cim T, Ludka FK, Martins WC, Reginato C, Parada E, Egea J, López MG, Tasca CI (2013b) Guanosine controls inflammatory pathways to afford neuroprotection of hippocampal slices under oxygen and glucose deprivation conditions. J Neurochem 126(4):437–450. https://doi.org/10.1111/jnc.12324

Dal-Cim T, Martins WC, Santos AR, Tasca CI (2011) Guanosine is neuroprotective against oxygen/glucose deprivation in hippocampal slices via large conductance Ca^2+-activated K+ channels, phosphatidilinositol-3 kinase/protein kinase B pathway activation and glutamate uptake. Neuroscience 183:212–220. https://doi.org/10.1016/j.neuroscience.2011.03.022

Dal-Cim T, Molz S, Egea J, Parada E, Romero A, Budni J, Martín de Saavedra MD, Barrio L, Tasca CI, López MG (2012) Guanosine protects human neuroblastoma SH-SY5Y cells against mitochondrial oxidative stress by inducing heme oxigenase-1 via PI3K/Akt/GSK-3β pathway. Neurochem Int 61(3):397–404. https://doi.org/10.1016/j.neuint.2012.05.021

de Lau LM, Breteler MM (2006) Epidemiology of Parkinson's disease. Lancet Neurol 5(6):525–535. https://doi.org/10.1016/S1474-4422(06)70471-9

Dias V, Junn E, Mouradian MM (2013) The role of oxidative stress in Parkinson's disease. J Parkinsons Dis 3(4):461–491. https://doi.org/10.3233/JPD-130230

Dobrachinski F, da Rosa Gerbatin R, Sartori G, Ferreira Marques N, Zemolin AP, Almeida Silva LF, Franco JL, Freire Royes LF, Rechia Fighera M, Antunes Soares FA (2017) Regulation of mitochondrial function and glutamatergic system are the target of guanosine effect in traumatic brain injury. J Neurotrauma 34(7):1318–1328. https://doi.org/10.1089/neu.2016.4563

Egea J, Rosa AO, Sobrado M, Gandía L, López MG, García AG (2007) Neuroprotection afforded by nicotine against oxygen and glucose deprivation in hippocampal slices is lost in alpha7 nicotinic receptor knockout mice. Neuroscience 145(3):866–872. https://doi.org/10.1016/j.neuroscience.2006.12.036

Garver DL, Cedarbaum J, Maas JW (1975) Blood-brain barrier to 6-hydroxydopamine: uptake by heart and brain. Life Sci 17(7):1081–1084

Glinka YY, Youdim MB (1995) Inhibition of mitochondrial complexes I and IV by 6-hydroxydopamine. Eur J Pharmacol 292(3–4):329–332

Goedert M, Spillantini MG, Del Tredici K, Braak H (2013) 100 years of Lewy pathology. Nat Rev Neurol 9(1):13–24. https://doi.org/10.1038/nrneurol.2012.242

Herraiz T, Galisteo J (2015) Hydroxyl radical reactions and the radical scavenging activity of β-carboline alkaloids. Food Chem 172:640–649. https://doi.org/10.1016/j.foodchem.2014.09.091

Hong SJ, Zhang D, Zhang LH, Yang P, Wan J, Yu Y, Wang TH, Feng ZT, Li LH, Yew DTW (2015) Expression of dopamine transporter in the different cerebral regions of methamphetamine-dependent rats. Hum Exp Toxicol 34(7):707–717. https://doi.org/10.1177/0960327114555929

Kostrzewa RM, Jacobowitz DM (1974) Pharmacological actions of 6-hydroxydopamine. Pharmacol Rev 26(3):199–288

Lanznaster D, Dal-Cim T, Piermartiri TC, Tasca CI (2016) Guanosine: a neuromodulator with therapeutic potential in brain disorders. *Aging Dis* 7(5):657–679. https://doi.org/10.14336/AD.2016.0208

Liu Y, Peterson DA, Kimura H, Schubert D (1997) Mechanism of cellular 3-(4,5-dimethylthiazol-2-yl)-2,5-diphenyltetrazolium bromide (MTT) reduction. J Neurochem 69(2):581–593

Lowry OH, Rosebrough NJ, Farr AL, Randall RJ (1951) Protein measurement with the Folin phenol reagent. J Biol Chem 193(1):265–275

Magalingam KB, Radhakrishnan A, Haleagrahara N (2014) Protective effects of flavonol isoquercitrin, against 6-hydroxy dopamine (6-OHDA)-induced toxicity in PC12 cells. BMC Res Notes 7:49. https://doi.org/10.1186/1756-0500-7-49

Massari CM, Castro AA, Dal-Cim T, Lanznaster D, Tasca CI (2016) In vitro 6-hydroxydopamine-induced toxicity in striatal, cerebrocortical and hippocampal slices is attenuated by atorvastatin and MK-801. Toxicol in Vitro 37:162–168. https://doi.org/10.1016/j.tiv.2016.09.015

Massari CM, López-Cano M, Núñez F, Fernández-Dueñas V, Tasca CI, Ciruela F (2017) Antiparkinsonian efficacy of guanosine in rodent models of movement disorder. Front Pharmacol 8:700. https://doi.org/10.3389/fphar.2017.00700

Mizuno Y, Ohta S, Tanaka M, Takamiya S, Suzuki K, Sato T, Oya H, Ozawa T, Kagawa Y (1989) Deficiencies in complex I subunits of the respiratory chain in Parkinson's disease. Biochem Biophys Res Commun 163(3):1450–1455

Molz S, Dal-Cim T, Budni J, Martín-de-Saavedra MD, Egea J, Romero A, del Barrio L, Rodrigues ALS, López MG, Tasca CI (2011) Neuroprotective effect of guanosine against glutamate-induced cell death in rat hippocampal slices is mediated by the phosphatidylinositol-3 kinase/Akt/ glycogen synthase kinase 3β pathway activation and inducible nitric oxide synthase inhibition. J Neurosci Res 89(9):1400–1408. https://doi.org/10.1002/jnr.22681

Molz S, Decker H, Dal-Cim T, Cremonez C, Cordova FM, Leal RB, Tasca CI (2008) Glutamate-induced toxicity in hippocampal slices involves apoptotic features and p38 MAPK signaling. Neurochem Res 33(1):27–36. https://doi.org/10.1007/s11064-007-9402-1

Mosmann T (1983) Rapid colorimetric assay for cellular growth and survival: application to proliferation and cytotoxicity assays. J Immunol Methods 65(1–2):55–63

Navarro A, Boveris A, Bández MJ, Sánchez-Pino MJ, Gómez C, Muntané G, Ferrer I (2009) Human brain cortex: mitochondrial oxidative damage and adaptive response in Parkinson disease and in dementia with Lewy bodies. Free Radic Biol Med 46(12):1574–1580. https://doi.org/10.1016/j.freeradbiomed.2009.03.007

Parker WD, Boyson SJ, Parks JK (1989) Abnormalities of the electron transport chain in idiopathic Parkinson's disease. Ann Neurol 26(6):719–723. https://doi.org/10.1002/ana.410260606

Perier C, Vila M (2012) Mitochondrial biology and Parkinson's disease. Cold Spring Harb Perspect Med 2(2):a009332. https://doi.org/10.1101/cshperspect.a009332

Piermartiri TC, Vandresen-Filho S, de Araújo Herculano B, Martins WC, Dal'agnolo D, Stroeh E et al (2009) Atorvastatin prevents hippocampal cell death due to quinolinic acid-induced seizures in mice by increasing Akt phosphorylation and glutamate uptake. Neurotox Res 16(2):106–115. https://doi.org/10.1007/s12640-009-9057-6

Poewe W, Seppi K, Tanner CM, Halliday GM, Brundin P, Volkmann J, Schrag AE, Lang AE (2017) Parkinson disease. Nat Rev Dis Primers 3:17013. https://doi.org/10.1038/nrdp.2017.13

Przedborski S (2017) The two-century journey of Parkinson disease research. Nat Rev Neurosci 18(4):251–259. https://doi.org/10.1038/nrn.2017.25

Schober A (2004) Classic toxin-induced animal models of Parkinson's disease: 6-OHDA and MPTP. Cell Tissue Res 318(1):215–224. https://doi.org/10.1007/s00441-004-0938-y

Segura-Aguilar J, Kostrzewa RM (2015) Neurotoxin mechanisms and processes relevant to Parkinson's disease: an update. Neurotox Res 27(3):328–354. https://doi.org/10.1007/s12640-015-9519-y

Su C, Elfeki N, Ballerini P, D'Alimonte I, Bau C, Ciccarelli R, Caciagli F, Gabriele J, Jiang S (2009) Guanosine improves motor behavior, reduces apoptosis, and stimulates neurogenesis in rats with parkinsonism. J Neurosci Res 87(3):617–625. https://doi.org/10.1002/jnr.21883

Thomaz DT, Dal-Cim TA, Martins WC, Cunha MP, Lanznaster D, de Bem AF, Tasca CI (2016) Guanosine prevents nitroxidative stress and recovers mitochondrial membrane potential disruption in hippocampal slices subjected to oxygen/glucose deprivation. Purinergic Signal 12(4):707–718. https://doi.org/10.1007/s11302-016-9534-3